

# CASCADE RESONANCE PROPERTIES FROM CHARM BARYON DECAYS AT *BABAR*

*V. Ziegler*  
Stanford Linear Accelerator Center  
Menlo Park, CA 94025  
U.S.A.

## Abstract

We present studies of hyperon and hyperon resonance production in charm baryon decays at *BABAR*. Two-body decay spin formalisms are extended to three-body final states and are used to study  $\Xi(1530)^0$  production in  $\Lambda_c^+$  decay. Similarly, the properties of the  $\Xi(1690)^0$  are extracted from a detailed isobar model analysis of the  $\Lambda_c^+ \rightarrow \Lambda K_S K^+$  Dalitz plot.

## 1 Introduction

Although considerable advances have been made in baryon spectroscopy over the past decade, there has been very little improvement in our knowledge of cascade resonances since 1988 [2]. The  $\Xi(1690)$  has been observed in the  $\Lambda\bar{K}$ ,  $\Sigma\bar{K}$  and  $\Xi\pi$  final states with various degrees of certainty. Its quantum numbers have not yet been measured. The  $\Xi(1530)$  has primarily been seen via its decay to  $\Xi\pi$ , however its spin-parity remains uncertain.

## 2 The $\Xi(1530)^0$ from $\Lambda_c^+ \rightarrow \Xi^-\pi^+K^+$ Decay

The  $\Xi(1530)^0$  resonance is observed in the  $\Xi^-\pi^+$  system produced in the decay  $\Lambda_c^+ \rightarrow (\Xi^-\pi^+)K^+$ . The data sample analyzed corresponds to a total integrated luminosity of  $\sim 230 \text{ fb}^{-1}$  [3, 4].

The Dalitz plot for  $\Lambda_c^+ \rightarrow \Xi^-\pi^+K^+$  is dominated by the contribution from  $\Lambda_c^+ \rightarrow \Xi(1530)^0K^+$ . The efficiency-corrected projection of the  $\Xi^-\pi^+$  invariant mass for the  $\Lambda_c^+$  signal region is shown in Fig. 1(a). The Dalitz plot (Fig. 1(d)) shows evidence for only one resonant structure. A clear band can be seen at the nominal mass squared of the  $\Xi(1530)^0 \rightarrow \Xi^-\pi^+$ .

Spin information for the  $\Xi(1530)$  is obtained using Legendre polynomial moments ( $P_L(\cos\theta_{\Xi^-})$ , where  $\cos\theta_{\Xi^-}$  is the  $\Xi^-$  helicity cosine). The  $\sqrt{10}P_2(\cos\theta_{\Xi^-})$  moment of the  $(\Xi^- \pi^+)$  system invariant mass distribution for the  $\Lambda_c^+$  signal region indicates that spin 3/2 is clearly favored (see Fig. 1(b)), whereas the  $7/\sqrt{2}P_4(\cos\theta_{\Xi^-})$  moment is consistent with being flat (Fig. 1(c)) implying that spin 5/2 is ruled out. Schlein *et al.* [5] showed that  $J^P = 3/2^+$  or  $J^P = 5/2^-$  and claimed  $J > 3/2$  not required, thereby concluding that  $J^P = 3/2^+$  was favored by their data. The present analysis by establishing  $J = 3/2$  also establishes positive parity by implication.

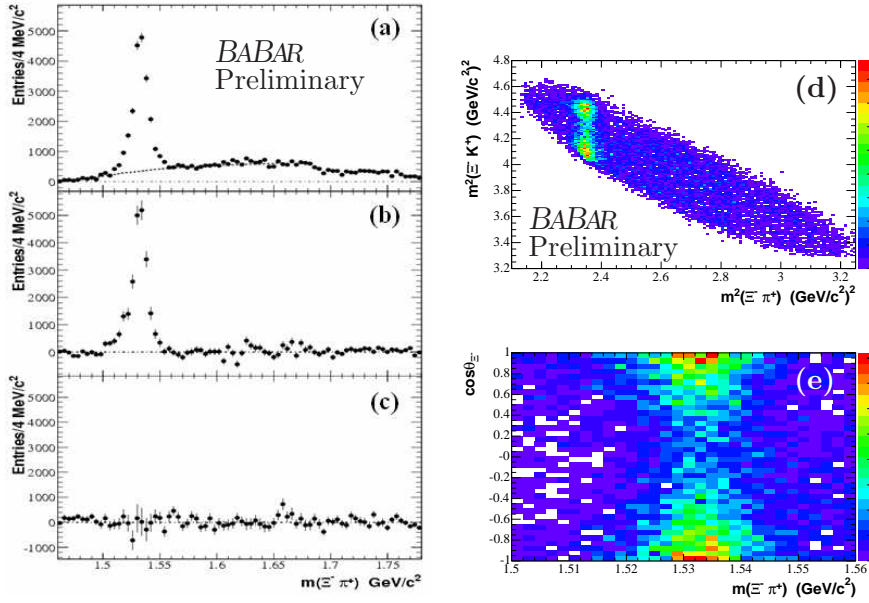


Figure 1: The  $\Lambda_c^+$ -mass-sideband-subtracted (a)  $m(\Xi^- \pi^+)$  projection, (b)  $\sqrt{10}P_2(\cos\theta_{\Xi^-})$  and (c)  $7/\sqrt{2}P_4(\cos\theta_{\Xi^-})$  moments of the  $\Xi^- \pi^+$  system invariant mass distribution, for the  $\Lambda_c^+$  signal region, after efficiency correction. In (a) the dashed curve represents the estimated background contribution in the  $\Xi(1530)$  region. (d) The Dalitz plot of  $m^2(\Xi^- K^+)$  versus  $m^2(\Xi^- \pi^+)$  for the  $\Lambda_c^+$  signal region. (e) The corresponding rectangular Dalitz plot for the  $\Xi(1530)^0$  mass region.

### 3 The $\Xi(1690)^0$ from $\Lambda_c^+ \rightarrow (\Lambda \bar{K}^0) K^+$ Decay

The  $\Xi(1690)^0$  is observed in the  $\Lambda \bar{K}^0$  system produced in the decay  $\Lambda_c^+ \rightarrow (\Lambda \bar{K}^0) K^+$ , where the  $\bar{K}^0$  is reconstructed via  $K_S \rightarrow \pi^+ \pi^-$ .

The data sample analyzed corresponds to a total integrated luminosity of  $\sim 200 \text{ fb}^{-1}$  [3,4]. The invariant mass spectrum of the resulting  $\Lambda_c^+$  candidates

before efficiency-correction and the  $\Lambda\bar{K}^0$  mass distribution corresponding to the  $\Lambda_c^+$  signal region are shown in Fig. 2(a) and (b), respectively. A clear peak is seen in the vicinity of the  $\Xi(1690)^0$ ; it should be noted that this signal is skewed significantly toward high mass.

The second and fourth order Legendre polynomial moments as a function of the mass of the  $(\Lambda K_S)$  system display no peaking structure at the position of the  $\Xi(1690)^0$ , which suggests that the  $\Xi(1690)^0$  spin is probably 1/2. However, the  $\Lambda$  helicity cosine ( $\cos\theta_\Lambda$ ) distribution is not flat in contrast to the expectation for a spin 1/2 to 1/2 transition. The Dalitz plot of  $\Lambda_c^+ \rightarrow \Lambda\bar{K}^0 K^+$  signal candidates is shown, without efficiency-correction, in Fig. 3(a). A clear band is observed in the mass-squared region of the  $\Xi(1690)^0$ , together with an accumulation of events in the  $\bar{K}^0 K^+$  threshold region; the latter is consistent with a contribution to the Dalitz plot due to the  $a_0(980)^+$  resonance. In contrast, the Dalitz plots corresponding to the  $\Lambda_c^+$  mass-sideband regions exhibit no structure [3].

The Dalitz plot of Fig. 3(b) is described in terms of an isobar model consisting of the coherent superposition of amplitudes characterizing  $(\Lambda a_0(980)^+)$  and  $(\Xi(1690)^0 K^+)$  decay of the  $\Lambda_c^+$ . The  $a_0(980)$  is known to couple to both  $\eta\pi$  and  $\bar{K}K$  and is characterized by the Flatté parametrization [6], while a Breit-Wigner function is used to describe the amplitude for the  $\Xi(1690)^0$ .

The intensity distribution at a point on the Dalitz plot is described by the squared modulus of the coherent superposition of these two amplitudes, assuming that the  $\Xi(1690)^0$  has spin 1/2, since the moment projections favor this choice. Fits to the Dalitz plot assuming spin 3/2 and 5/2 are poorer than for spin 1/2, and yield systematic failures in the description of the resulting  $\cos\theta_\Lambda$  and  $m(\Lambda K_S)$  projections [3]. The skewing of the  $\Lambda K_S$  invariant mass projection results from the interference between the  $a_0(980)^+$  and the  $\Xi(1690)^0$ . The actual  $\Xi(1690)^0$  signal is symmetric and smaller than the observed signal, because of significant interference effect [3].

## 4 Conclusions

The properties of the  $\Xi(1530)^0$  are studied using the decay  $\Lambda_c^+ \rightarrow \Xi^-\pi^+K^+$ . The spin of the  $\Xi(1530)$  is established as 3/2. The properties of the  $\Xi(1690)^0$  are extracted from fits to the  $\Lambda_c^+ \rightarrow \Lambda K_S K^+$  Dalitz plot. The hypothesis that the  $\Xi(1690)$  has spin 1/2 yields an excellent description of the data, whereas spin values of 3/2 and 5/2 result in poorer fit probabilities, and fail to reproduce the observed skewed  $\Xi(1690)$  lineshape.

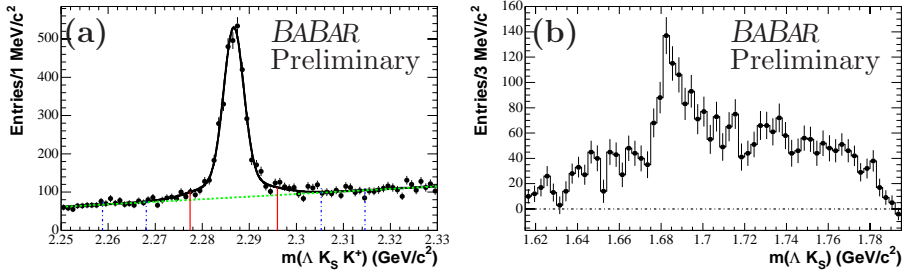


Figure 2: (a) The invariant mass distribution of uncorrected  $\Lambda_c^+ K_S K^+$  candidates in data. (b) The  $\Lambda_c^+$  mass-sideband-subtracted  $\Lambda_c^+ K_S$  invariant mass projection of uncorrected  $\Lambda_c^+ K_S K^+$  candidates.

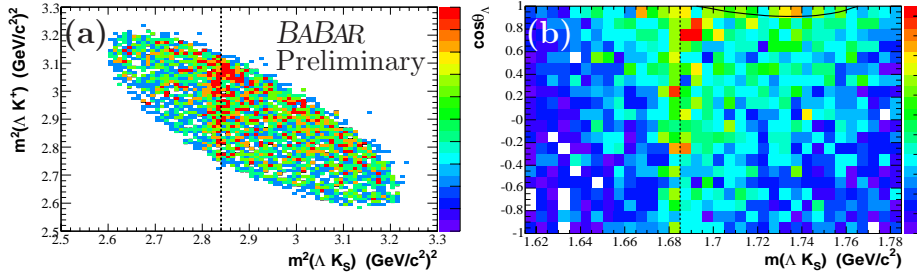


Figure 3: (a) The Dalitz plot for  $\Lambda_c^+ \rightarrow \Lambda \bar{K}^0 K^+$  corresponding to the  $\Lambda_c^+$  signal region indicated in Fig. 2. The dashed line indicates the nominal mass-squared region of the  $\Xi(1690)^0$ . (b) The rectangular Dalitz plot for  $\Lambda_c^+ \rightarrow \Lambda \bar{K}^0 K^+$  corresponding to the  $\Lambda_c^+$  signal region indicated in Fig. 2. The black curve corresponds to the  $a_0(980)^+$  pole position.

## References

- [1] B. Aubert *et al.*, Nucl. Instr. Meth. **A479**, 1 (2002).
- [2] W.-M. Yao *et al.* (PDG2006), J.Phys. G:Nucl.Part.Phys. **33**, 1 (2006).
- [3] Veronique Ziegler, *Ph.D. Thesis*, SLAC-R-868 (2007).
- [4] The use of charge conjugate states is implied throughout.
- [5] P. E. Schlein *et al.*, Phys. Rev. Lett. **11**, 167 (1963); J. Button-Schafer *et al.*, Phys. Rev. **B142**, 883 (1966).
- [6] S. M. Flatté, Phys. Lett. **B63**, 224 (1976).